Catal Lett (2013) 143:276–281
DOI 10.1007/s10562-012-0956-4

Hydrogenation of Alkenes with Rhodium Nanoparticles Supported on SBA-15

Nayanmoni Bhorali · Jatindra Nath Ganguli

Received: 10 November 2012 / Accepted: 17 December 2012 / Published online: 9 January 2013

Abstract Rhodium nanoparticles were prepared by chemical reduction of $RhCl_3 \cdot 3H_2O$ in presence of polyvinyl pyrrolidone and then immobilized on SBA-15 by impregnation. The catalyst was used for hydrogenation of unsaturated hydrocarbons at room temperature. The progress of the reaction was monitored by GC–MS and 100 % conversion was achieved in all cases.

Keywords Mesoporous silicates · Rh-SBA-15 · Rhodium-nanoparticles · Hydrogenation

1 Introduction

The overall performance and activity of catalyst and selectivity are ruled by size and morphology of active metals [1–3]. Though metal nanoparticles with different sizes and morphologies have been synthesized, yet their successful application in catalysis is a big challenge for chemists. The main disadvantage in this regard is the possibility of agglomeration and sintering of the nanoparticles under drastic catalytic reaction conditions. Hence it is important to support the nanoparticles effectively on solid and stable materials which would prevent agglomeration and deactivation. Interest in the synthesis and properties of colloidal metal nanoparticles has been increasing because of their unique properties and applications as catalyst. Two main aspects in the synthesis of the metal colloid nanoparticles are to control the growth of metal nanoparticles in terms of particle size, particle size distribution and structure of the particle and the stabilization of the colloids. Among various techniques, chemical reduction techniques are important for the synthesis of nanoparticles, because these methods can be applied under simple and mild conditions and can also be used to prepare nanoparticles on a large scale [4]. Though transition metal nanoparticles act as good catalyst for many organic synthesis, the liquid suspensions of metal nanoparticles in catalysis is difficult to separate and recycle. Our work focuses on immobilization of metal nanoparticles on mesoporous solid support materials. Mevellec et al. [5] reported a synthetic method for preparation of rhodium nanoparticles by addition of silica to a pre stabilized rhodium aqueous colloidal suspension. Although Somorjai and coworkers [6] also reported synthesis of Rh nano particles and ethylene hydrogenation, their method is high temperature synthesis and the catalysis is also at high temperature and pressure, in comparison our method reported in this paper is simple, starting from $RhCl_3$, room temperature synthesis of Rh nano particles and liquid phase heterogeneous hydrogenation of various alkenes at low pressure and room temperature.

2 Experimental: Materials and Methods

Rhodium chloride hydrate was obtained from Arora Matthey, sodium borohydride and the alkenes were purchased from Merck and were used without further purification. Tetraethylorthosilicate (TEOS) and block polymer—$EO_{20}PO_{70}EO_{20}$ were purchased from Aldrich.

Growth of the rhodium nanoparticles by sodium borohydride reduction in PVP was monitored by absorption spectroscopy. UV–Visible spectroscopy was carried out in a double beam Hitachi (U-4100) spectrophotometer. Rh(0) sol was studied in 10 mm quartz cuvettes.

N. Bhorali · J. N. Ganguli (✉)
Department of Chemistry, Gauhati University, Gauhati, Assam, India
e-mail: jatin_ganguli_gu@yahoo.co.in

Powder XRD spectra were recorded on a Brucker D8 X-ray diffractometer from 5–75° 2θ using Cu-Kα source (λ = 1.54 Å). Low angle XRD spectra were recorded on a Rigaku X-ray diffractometer from 0.5–10° 2θ using Cu-Kα source (λ = 1.54 Å). The nitrogen adsorption and desorption isotherms were measured using Micromeritics Tristar 3000 system. Before adsorption, the samples were degassed at 250 °C for 3 h. Pore volume were derived from the isotherms using the Barrett–Joyner–Halenda (BJH) method. Scanning electron microscopy (SEM) images and energy dispersive X-ray Spectroscopy (EDX) were collected with JEOL, Model: JSM6390LV, operated at 15 kV. High resolution TEM images were recorded in JEOL JEM 2100 TEM instrument and operated at 200 kV. Aqueous suspension of the sample was prepared in dry carbon coated Cu-grid. Hydrogenation reactions were carried out under room temperature (27 °C) and 4 bar pressure in a Parr hydrogenation apparatus. The reaction was monitored by the volume of gas consumed (the pressure indicator in the Parr apparatus gradually falls down with the consumption of the H_2 gas) and using a Perkin Elmer GCMS (Clarus 600) with an Elite 5MS column (30 m, 250 μm i.d.).

2.1 Synthesis of SBA-15 Silica

The synthesis of mesoporous silica SBA-15 was done according to a previously reported procedure [7]. Pluronic P123 (4 g) was dissolved in 144 mL 2 M HCl solution with constant stirring at 308 K for 2 h. TEOS (9 mL) (TEOS/P123 = 2) was added to the solution with constant stirring at 308 K for 4 h. The mixture was aged for 12 h, transferred to a high pressure Teflon lined stainless steel autoclave and then heated at 373 K for 48 h. The white powder was recovered through filtration, washed with water and ethanol thoroughly and dried at 353 K for 12 h and finally calcined at 813 K for 3 h.

2.2 Synthesis of Aqueous Rhodium (0) Suspension: Polymer Stabilized Rh(0) Nanosols

To an aqueous solution of PVP (0.02 g/100 mL), sodium borohydride (0.1 g) was added. Then this solution was quickly added under vigorous stirring to an aqueous solution (100 mL) of precursor $RhCl_3 \cdot 3H_2O$ (0.1 g, 0.4×10^{-3} mol) to obtain an aqueous Rh(0) colloidal suspension. The reduction occurred instantaneously and was characterized by color change from red to black. Since complete reduction of Rh^{3+} to Rh(0) occurs, amount of Rh(0) is 0.04 g.

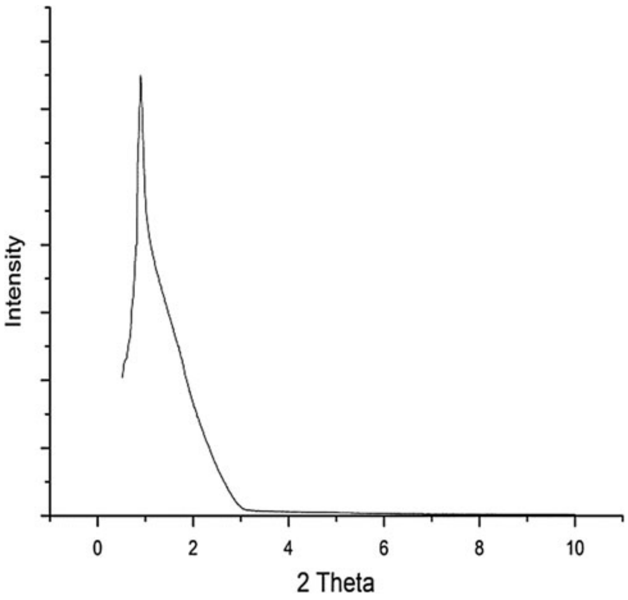

Fig. 1 Low angle XRD of Rh-SBA-15

2.3 Synthesis of the SBA-15 Supported Rhodium Nanoparticles

SBA-15 silica (1 g) was added under vigorous stirring to 50 mL of deionized water. After 2 h, the above prepared Rh(0) colloidal suspension was added under vigorous stirring to this suspension. The system was kept under stirring for 4 h. Then the content was filtered and the brown powder was washed several times with distilled water to eliminate the PVP and evaporated to dryness at 353 K (Fig. 1).

3 Results and Discussions

3.1 X-ray Diffraction Analysis

The calcined SBA-15 had an ordered hexagonal structure, as indicated by the intense (100), (110), and (200) reflection in the small angle region of powder X-ray diffraction pattern shown in Fig. 2. The intense (100) peak corresponds to a d spacing of 97 Å and this remained unchanged after the incorporation of rhodium nanoparticles. Other weak peaks found in 2θ range of 1°–3.5° correspond to the (110), (200) reflections indicating high degree of hexagonal mesoscopic structure.

The X-ray diffraction (XRD) pattern of Rhodium nanoparticle (Fig. 3) shows a diffuse “peak”. The diffraction angle of the peak is found nearly 2θ = 42.8°, which is consistent with the d-value of rhodium metal. A very broad signal at 2θ = 23° for amorphous SiO_2.

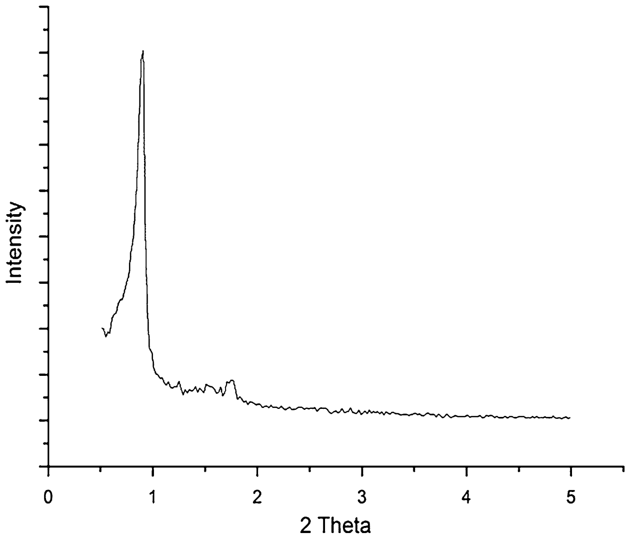

Fig. 2 Low angle XRD of SBA-15(Calcined)

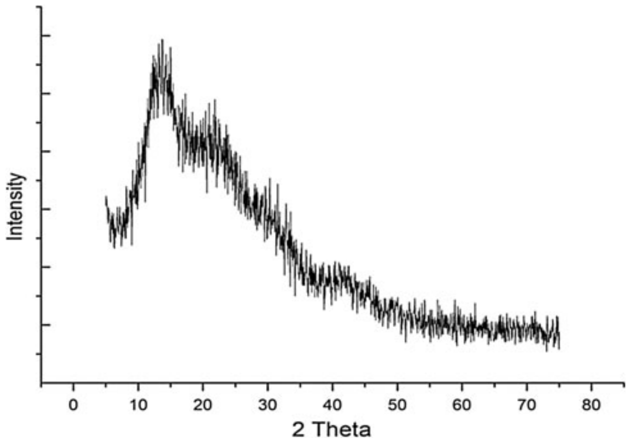

Fig. 3 High angle XRD of Rh nanoparticles

3.2 Nitrogen Absorption–Desorption

Figures 4 and 5 shows nitrogen adsorption desorption isotherm for SBA-15 and Rh-SBA-15 samples. The estimated textural parameters are compiled in Table 1.

All of the nitrogen adsorption/desorption isotherms are found to be of Type IV in nature as per the IUPAC nomenclature and exhibited a H1 hysteresis loop which is typical of mesoporous solid [8]. The adsorption branches of each isotherm showed a sharp inflection in the relative pressure range of about 0.60–0.68. This is a characteristic of capillary condensation [7]. The position of the inflection point is clearly related to a diameter in the mesopore range. The sharpness of these steps indicates the uniformity of the mesopore size distribution [8]. After Rh incorporation, the total pore volume decreases, while the average pore size is essentially unchanged. This suggests that the majority of the nanometer scaled void space of the host SBA-15 was still open, although a small portion of the mesoporous channels may be occupied by the Rh-nanoparticles which indicate the reduction in the surface area and the pore volume [9, 10].

3.3 UV–Visible Analysis

The amount of reducing agent required for complete conversion was determined with the help of UV–Visible analyser. To a 0.4 mM rhodium chloride solution containing 0.02 g/100 mL PVP, a 26 mM (0.1 g/100 mL) solution of reducing agent was added with constant stirring. The process of reduction at different $NaBH_4$ concentration was followed on the UV–Vis spectra as shown in Fig. 6. The peaks which are characteristic of the chloro-complexes of rhodium (225 and 198 nm) gradually disappeared and was accompanied by a gradual rise of the descending branch of the spectrum (in the range of 260–300 nm). In presence of excess of reducing agent the new peak, characteristic of Rh (0) nanoparticles appears at 194 nm. The curve shows that 1:1 $Rh^{3+}/NaBH_4$ is necessary for the complete reduction.

3.4 SEM Analysis

From the figure (Fig. 7) it can be concluded that the SBA-15 particles were cylindrical and freely distributed with some aggregation. The EDX shows the atomic percentage of Rh-nanoparticle as 2.3 %.

3.5 TEM Analysis

The morphology distributions of Rh nanoparticles on the surface of the SBA-15 were shown in the TEM image (Fig. 8). The image shows that the pore structure is regular with well-ordered arrays, and the metallic nanoparticles are well dispersed. The shape of the rhodium nanoparticles are spherical or quasi-spherical and are homogeneously dispersed. The Rh nanoparticles have a narrow size distribution in the range of 3–4 nm. The Rh particles are well separated with no agglomeration tendency. Histrogram in Fig. 9 shows the particle size distribution of the Rh-nanoparticles obtained from 209 particles from TEM image.

4 Catalytic Study

The SBA-15 supported Rh nanocatalyst previously described has been tested in the hydrogenation of various unsaturated compounds under mild conditions. In all cases, a total conversion of substrate has been observed. The amount of substrate was 1 mmol in all the cases; we have

Fig. 4 N_2 adsorption–desorption isotherm of SBA-15

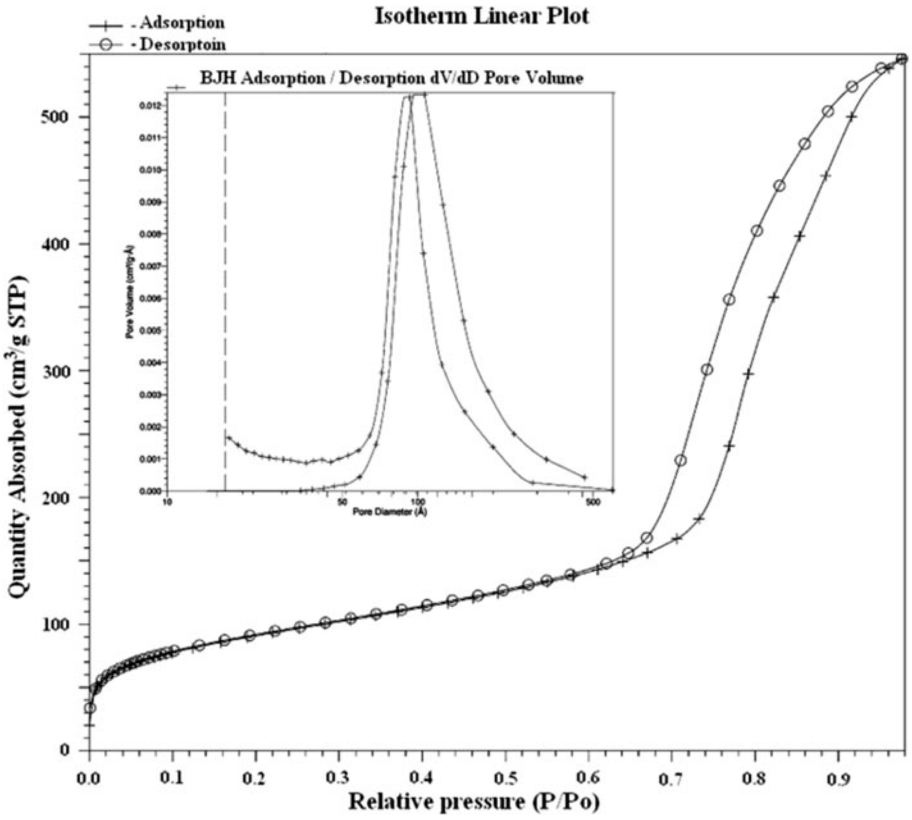

Fig. 5 N_2 adsorption–desorption isotherm of Rh-SBA-15

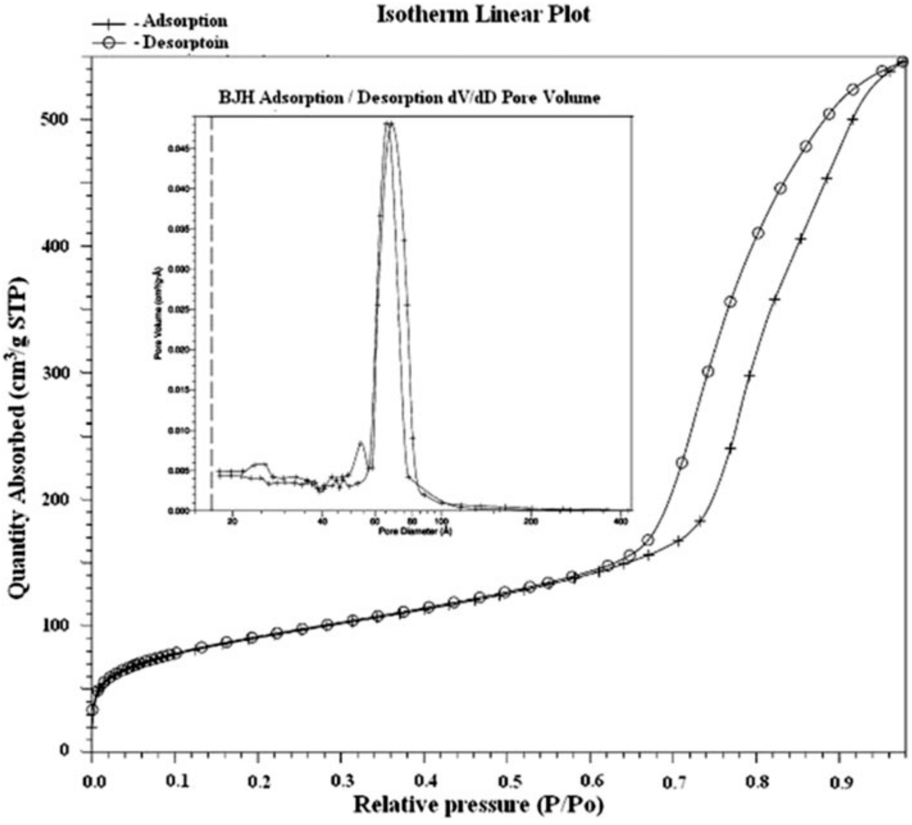

Table 1 Surface parameters of SBA-15 and Rh-SBA-15

Entry	BET surface area (m^2/g)	Pore volume (cm^3/g)	
		BJH adsorption	BJH desorption
SBA-15	720	0.85	0.86
Rh-SBA-15	320	0.81	0.80

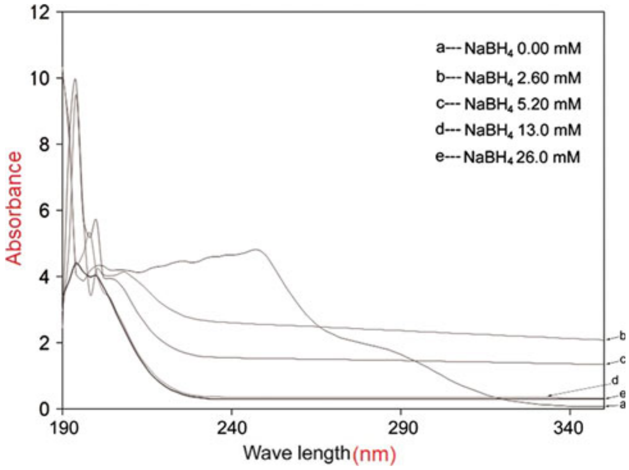

Fig. 6 Determination of amount of $NaBH_4$ for total reduction of Rh^{3+} by adsorption spectrophotometry

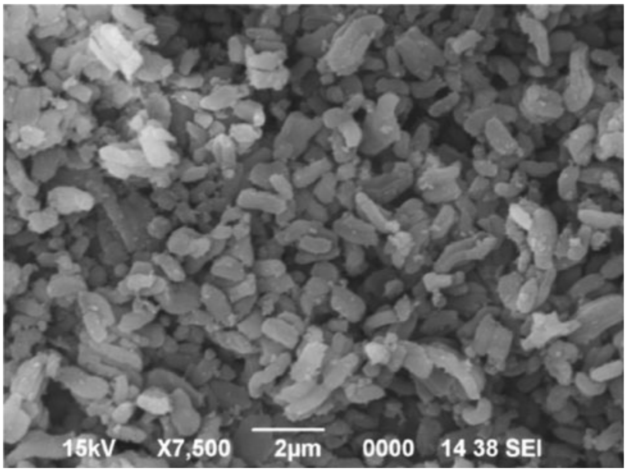

Fig. 7 SEM pictures of Rh-SBA-15

also observed by taking 10 mmol substrates keeping all other conditions same. But we have not observed noticeable change, except small change in time taken for complete conversion. Active sites were calculated as function of Rhodium-crystallite size from TEM. On the basis of active site TOF for hydrogenation of the alkenes were evaluated [11]

For comparison, we have tested 1-Hexene hydrogenation with Wilkinson catalyst $RhCl(PPh_3)_3$ under identical conditions. But it takes more time for complete conversion (Table 2).

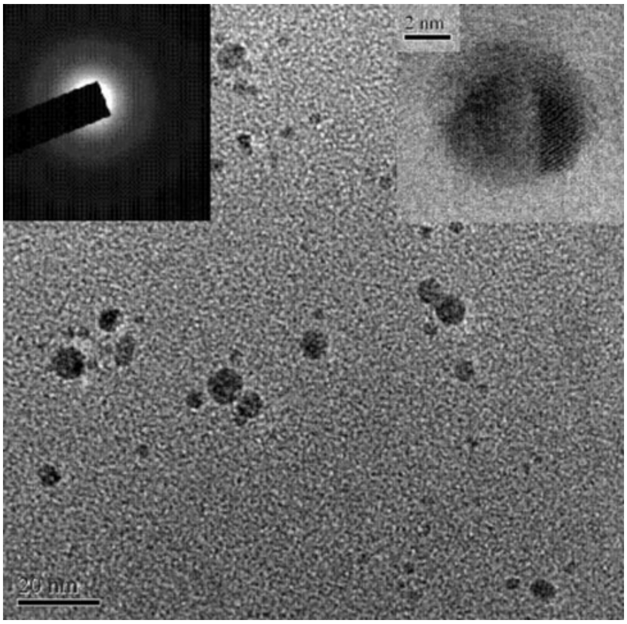

Fig. 8 TEM image of Rh-SBA-15

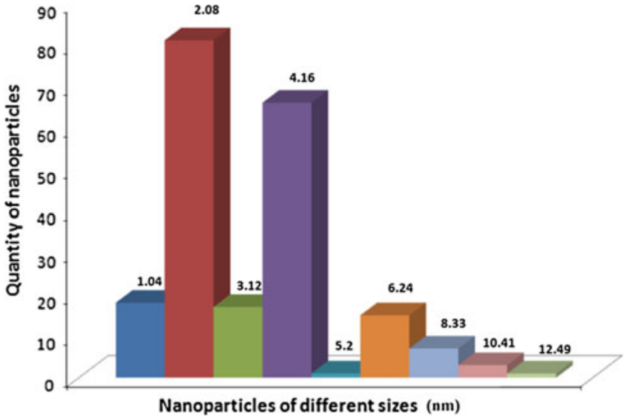

Fig. 9 Particle size distribution of Rh-nanoparticles

Recycling experiments have been investigated on catalytic systems. After each run, the catalyst was recovered by simple filtration and dried at 333 K before another run with new addition of substrate. Five run could be performed at least with no loss of activity. These results show no leaching of Rh nanoparticles during the catalytic reactions.

5 Conclusion

We have shown that an aqueous solution containing prestabilized Rh nanoparticles can be used easily for particle deposition onto SBA-15 through simple impregnation. The

Table 2 Catalytic activity in the hydrogenation of unsaturated hydrocarbons

Catalyst	Amount (g)	Reactant	Product	Time (h)	TOF
Rh-SBA-15	0.05	Cyclohexene	Cyclohexane[a]	0.05	11,582
Rh-SBA-15	0.02	Cyclohexene	Cyclohexane[a]	0.13	11,110
SBA-15	0.05	Cyclohexene	Cyclohexane[a]	0.33	
Rh-SBA-15	0.05	10 mmol of Cyclohexene	Cyclohexane[a]	0.35	16,546
Rh-SBA-15	0.05	Geraniol	Citronellol[a]	0.116	4,992
Rh-SBA-15	0.02	Geraniol	Citronellol[a]	0.2	7,221
Rh-SBA-15	0.05	10 mmol of Geraniol	Citronellol[a]	0.266	21,771
Rh-SBA-15	0.05	1-Hexene	Haxane[a]	0.10	5,791
Rh-SBA-15	0.02	1-Hexene	Haxane[a]	0.20	7,221
SBA-15	0.05	1-Hexene	1-Hexene	24	
Rh-SBA-15	0.05	10 mmol of 1-Hexene	Haxane[a]	0.166	34,887
Rh-SBA-15	0.05	Styrene	Ethylbenzene[a]	0.083	6,977
Rh-SBA-15	0.02	Styrene	Ethylbenzene[a]	0.166	8,700
Rh-SBA-15	0.05	10 mmol of styrene	Ethylbenzene[a]	0.166	34,887
Rh-SBA-15	0.05	Benzene	Cyclohexane[a]	0.116	4,992
Rh-SBA-15	0.02	Benzene	Cyclohexane[a]	2	722
*Rh-SBA-15	0.05	Phenol	Cyclohexanol[a]	2	289
*Rh-SBA-15	0.02	Phenol	Cyclohexanol[b] Cyclohexanone[b]	4	361
$RhCl(PPh_3)_3$	0.10	1-Hexene	Hexane[a]	19	

*water as solvent, others methanol as solvent, [a] 100 % conversion, [b] 50 % conversion

so-obtained SBA-15 supported rhodium nanoparticles displayed an unexpected activity for hydrogenation of various unsaturated hydrocarbons and could be reused for several times without significant loss of activity.

Acknowledgments The authors are thankful to Department of Chemistry, Gauhati University, IISc, Bangalore, NEHU, Shillong for different scientific analysis.

References

1. Somorjai GA, Borodko YG (2001) Catal Lett 76:1
2. Rioux RM, Song H, Grass M, Habas S, Niesz K, Hoefelmeyer JD, Yang P, Somorjai GA (2006) Top Catal 39:167
3. Guezi L, Peto G, Beck A, Paszti Z (2004) Catalysis 29:129
4. Tan Y, Dai X, Li Y, Zhu D (2003) J Mater Chem 13:1069
5. Mevellec V, Nowieki A, Roucoux A, Dujardin C (2006) New J Chem 30:1214
6. Zhang Y, Grass ME, Habas SE, Tao F, Zhang T, Yang P, Somorjai GA (2007) J Phys Chem C 111:12243
7. King KSW, Everett DH, Haul RAW, Moscow L, Pierotti RA, Rouqurrol J, Siemieniewska T (1985) Pure Appl Chem 57:603
8. Gregg SJ, Sing KSW (1982) Academic adsorption. Surface Area and Porosity Press, New York
9. Kruk M, Jaroniec M, Sayari A (1997) Langmuir 13:2499
10. Yang CM, Liu P, Ho Y, Chiu CY, Chau K (2003) Chem Mater 15:275
11. Bernadett V, Zoltan K, Lajos T, Bela P (2002) Chem Mater 14: 2882–2888